Dyes and Pigments 95 (2012) 455–464

Contents lists available at SciVerse ScienceDirect

Dyes and Pigments

journal homepage: www.elsevier.com/locate/dyepig

Synthesis and optical properties of NLO chromophores containing an indoline donor and azo linker

Mohamed Ashraf [a], Ayele Teshome [b], Andrew J. Kay [a,*], Graeme J. Gainsford [a], M. Delower H. Bhuiyan [a], Inge Asselberghs [b], Koen Clays [b]

[a] Photonics, Industrial Research Ltd., P.O. Box 31-310, Lower Hutt 5040, New Zealand
[b] Department of Chemistry, University of Leuven, Celestijnenlaan 200D, B-3001 Leuven, Belgium

ARTICLE INFO

Article history:
Received 7 November 2011
Received in revised form
22 February 2012
Accepted 13 April 2012
Available online 13 June 2012

Keywords:
Nonlinear optics
Chromophore synthesis
Hyperpolarizability
Hyper-Raleigh scattering
Azo dyes
Solvatochromism

ABSTRACT

A suite of new nonlinear optical chromophores containing an indoline donor and azo linker has been synthesized in high yields. The methodology used allows for the incorporation of various acceptor systems, the ready isolation of the target compounds and access to materials with excellent thermal stabilities (*viz* = T_d 220–270 °C). The first hyperpolarizabilities of the compounds were measured by hyper-Raleigh scattering and all were found to have an excellent response. The highest value measured was 1640 × 10^{-30} esu in DMF at 800 nm for a chromophore containing the well-known TCF acceptor system. Based on data obtained in this and other studies, there is evidence that chromophores containing indoline donors are capable of providing compounds with molecular NLO responses higher than those containing donors derived from *N*,*N*-disubstituted anilines.

1. Introduction

Materials having large second-order nonlinear optic (NLO) properties are in demand due to their potential applications in photonic devices and optical information processing [1–3]. At a fundamental level, organic push–pull NLO chromophores contain electron-donor and electron-acceptor groups at opposite ends of a π-conjugated spacer [4], and the vast majority of known organic NLO compounds utilize olefinic or aromatic linkers in the π-conjugated bridge. Many examples of different conjugated interconnects are known and vary from either open chain or ring-locked polyenes to various aromatic (heterocyclic) systems [5]. Furthermore, a significant number of organic compounds with large molecular NLO responses contain *N*,*N*-disubstituted anilines as this nucleus is an excellent electron donor, and because a vast array of substituents – some of which permit tethering – can be attached to the amine nitrogen atom. Coupled with the emergence of 4,5,5-trimethyl-3-cyano-2(5*H*)-furanylidenepropanedinitrile (TCF) [6] and its derivatives as powerful acceptors, the past decade has seen a number of steady improvements to the basic design of NLO chromophores. Indeed compounds containing an aniline-based donor, a π-conjugated interconnect of *c.* 6–12 carbon atoms and TCF as acceptor have become almost ubiquitous as core NLO materials and have been shown to have high molecular NLO responses [7]. Nonetheless, while these compounds have excellent electro-optic properties a number of other factors must be satisfied before an organic NLO material can be considered viable for device applications [8–11]. These include having high thermal and photochemical stabilities, being processable in a range of solvents, being optically transparent at the operating wavelength(s) and being amenable to large scale preparation. While a number of approaches have been made to address these challenges, one option is to incorporate an azo group in the conjugated interconnect instead of an olefinic linker. Azo based donor-π-acceptor systems such as this have been extensively investigated, with many showing improved optical nonlinearities and thermal stabilities when compared to their olefinic analogues [12]. Another advantage of using an azo linker is that the compounds prepared can also be studied for further applications as azobenzene/azo-heterocycle containing compounds have been the subject of intensive research in optical switching [13] and digital and holographic storage applications [14,15].

Organic NLO chromophores containing an azo linker and a donor based on *N*,*N*-dialkyl anilines are known and possess high molecular hyperpolarizabilities. Such molecules are perhaps best

* Corresponding author. Tel.: +64 4 931 3210; fax: +64 4 931 3306.
E-mail address: a.kay@irl.cri.nz (A.J. Kay).

0143-7208/$ – see front matter © 2012 Elsevier Ltd. All rights reserved.
http://dx.doi.org/10.1016/j.dyepig.2012.04.022

exemplified by compound **1** which has been reported to have a first hyperpolarizability value, β, of 682×10^{-30} and a static value (β_0) of 343×10^{-30} esu using data obtained in DMSO solutions at 800 nm [16]. In addition, we have recently described the preparation of a series of NLO compounds containing donors based on an indoline nucleus [17]. These compounds also have high NLO figures of merit with the most effective compound, **2**, having a β value of 1485×10^{-30} esu and β_0 value of 815×10^{-30} esu when measured at 800 nm in chloroform; the values are 1175×10^{-30} esu and 645×10^{-30} esu respectively for measurements obtained in DMSO. The likely reason for the superior performance of indoline-based compound **2** over compound **1** is due to the lower degree of aromaticity in the conjugated bridge between the donor and the acceptor. In accordance with this observation, Perez-Moreno et al. reported that for similar compounds the magnitude of the hyperpolarizability can breach the apparent limit found for similar molecules by modulating the degree of aromatic stabilization energy in the units that make up the conjugated interconnect [18]. Given these results it suggests that not only are azo compounds capable of yielding molecules with large NLO responses, but the use of indoline-based donors (as opposed to aniline-based) allows access to compounds with high first hyperpolarizabilities. Thus, it is a logical progression to target new chromophores containing indoline donors and azo linkers (e.g. **3**) as potentially interesting NLO materials. In this paper we report the syntheses and properties of a series of such compounds that exploit the electron rich indoline core as the donor component and to which a reactive diazonium salt can be directly coupled.

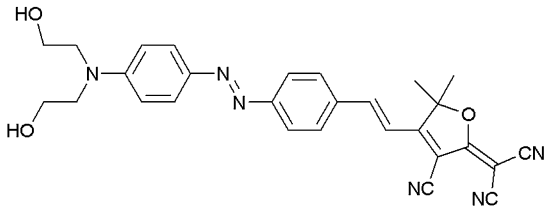

1

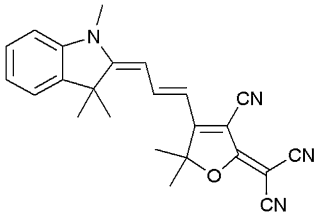

2

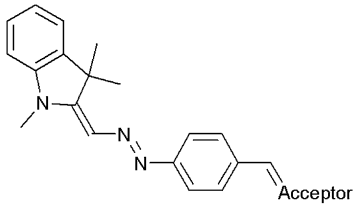

3

2. Experimental

2.1. Reagents and procedures

Commercially available reagents were obtained from Aldrich and were used without additional purification. The solvents used were of analytical grade and were also used without further purification. Column chromatography was carried out using gravity feed column techniques on Merck silica gel type 9385 (230–400 mesh) with the stated solvent systems. Analytical thin-layer chromatography (TLC) analyses were performed on pre-coated plates (Merck aluminium sheets, silica gel 60F 254, 0.2 mm). Visualisation of compounds was achieved by illumination under ultraviolet light (254 nm).

2.2. Measurements and instrumentation

Melting points were recorded with an *EZ-Melt* automated melting point apparatus and are uncorrected. ^{1}H and ^{13}C NMR spectra were recorded on a Bruker AVANCE 300 MHz or 500 MHz spectrometer and proton multiplicities are defined by the usual notations. Accurate mass measurements were made on a Micromass Q-Tof Premier Mass Spectrometer operating in the positive ion mode. The UV–Visible (UV–Vis) absorption spectra were recorded by a Perkin–Elmer Lambda 900 spectrometer at room temperature. Hyper-Rayleigh scattering (HRS) measurements were performed at 800 nm in both THF and DMF. Crystal violet dissolved in methanol was used as an octupolar external reference ($\beta_{xxx} = 338 \times 10^{-30}$ esu at 800 nm). For all of the HRS measurements, a series of dilute solutions were measured and compared to the reference concentration series. To correct for the differences in the solvent between the chromophores and the reference compound, local field correction factors were applied $[(n^2 + 2)/3]^3$ where n is the refractive index of the solvent at the sodium D line, with n(DMF) = 1.43, n(THF) = 1.41 and n(MeOH) = 1.32. The calculations of the dynamic first hyperpolarizability were performed by taking the ratio of the slopes of the sample and the reference compound. For dynamic first hyperpolarizability values obtained at 800 nm it is necessary to consider the appropriate tensor components (dipolar versus octupolar geometry) as the reference compound crystal violet is octupolar whereas the chromophores under investigation are dipolar. The static first hyperpolarizability is derived from the simple two-level model as previously described [19]. The apparatus and experimental procedures for the HRS measurements are exactly the same as described before [20].

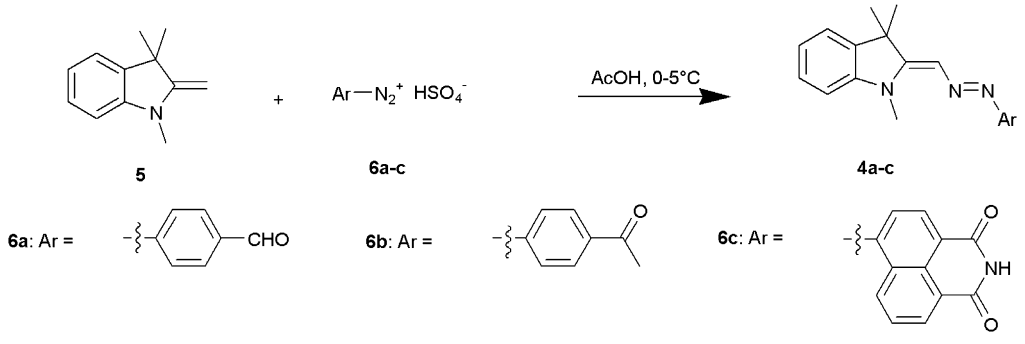

Scheme 1. Synthesis of the chromophores **4a–c**.

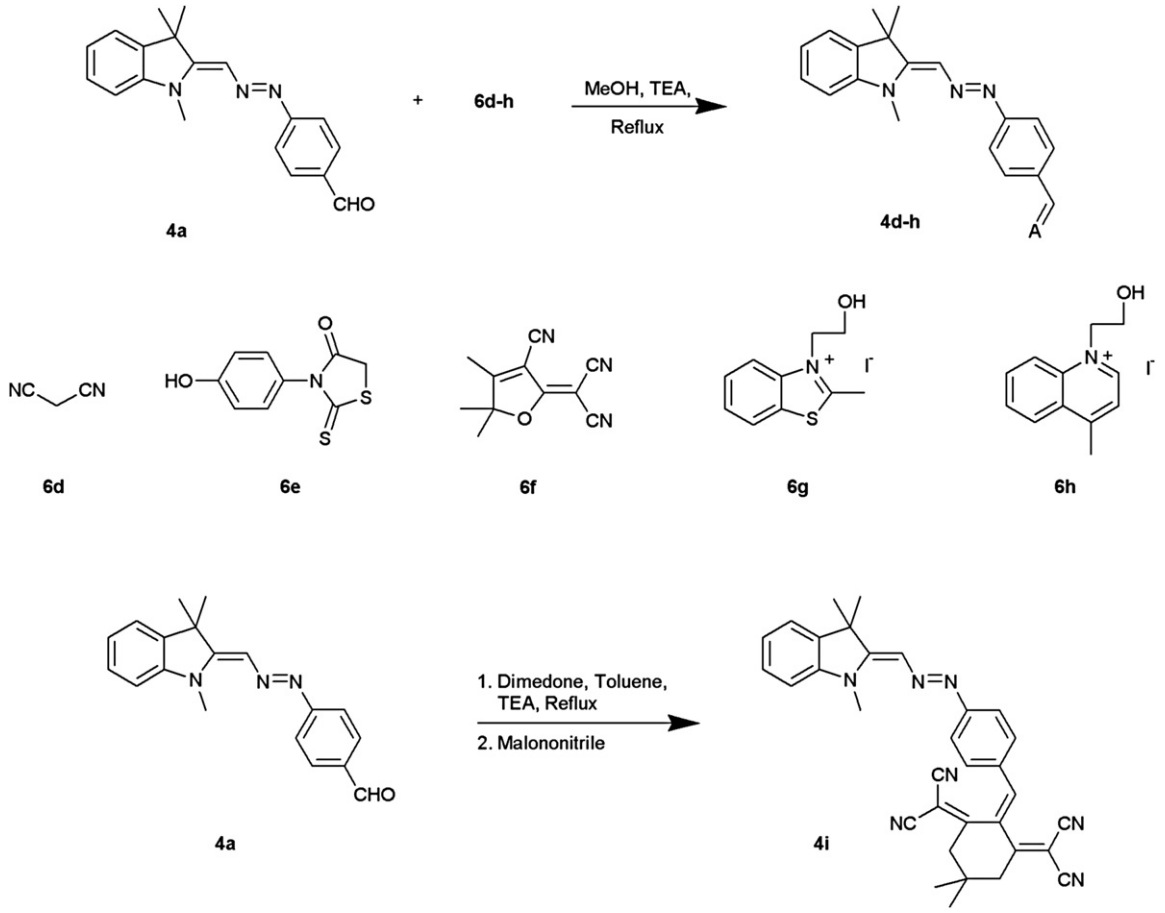

Scheme 2. Methodology used to prepare chromophores **4d**–**i**.

2.3. Preparation of chromophores

The methods used to synthesis the chromophores are shown in Schemes 1 and 2. 4-Aminobenzaldehyde and compounds **6e**–**h** were prepared according to the literature procedures [21].

2.4. Preparation of compounds *4a*–*c*. General diazotisation procedure

To conc. sulphuric acid (4 mL) was added the appropriate aryl amine (2.5 mmol) and the reaction mixture cooled to 0–5 °C. A solution of sodium nitrite (206 mg, 3 mmol) in 2 mL of water was then slowly added and the reaction stirred at 0–5 °C for 30 min. To this was added a solution of 1,3,3-trimethyl-2-methyleneindoline **5** (336 mg, 2 mmol) in 10 mL of glacial acetic acid and the solution stirred for 2 h and allowed to gradually warm to room temperature. The mixture was then poured into water and neutralized with aqueous sodium carbonate. The resulting precipitate was filtered, washed with water, dried, and recrystallized from ethanol to give the product as a deeply coloured solid.

2.4.1. 4-[(1,3,3-Trimethyl-1,3-dihydro-indol-2-ylidenemethyl)-azo]-benzaldehyde (*4a*)

Red solid (82%), m.p. 130 °C (Found: MH^+ *m*/*z* 306.1599 $C_{19}H_{19}N_3O$ requires MH^+ *m*/*z* 306.1606; Δ = 2.3 ppm). ^1H NMR (d_6-DMSO) δ 9.97 (s, 1H), 7.96 (d, *J* 9 Hz, 2H), 7.69 (d, *J* 9 Hz, 2H), 7.56 (s, 1H), 7.48 (t, *J* 5 Hz, 1H), 7.22 (d, *J* 3 Hz, 1H), 7.30 (d, *J* 9 Hz, 1H), 7.10 (t, *J* 9 Hz, 1H), 3.46 (s, 3H), 1.72 (s, 6H). ^{13}C NMR (d_6-DMSO) δ 21.1, 29.0, 29.1, 30.3, 47.8, 48.6, 108.4, 109.5, 121.0, 121.2, 121.8, 122.4, 123.0, 23.2, 129.4, 130.0, 131.3, 134.2, 140.2, 144.1, 158.4, 168.9, 192.3. λ_{max} (DMF) 471, $\log_{10}\varepsilon$ 4.55.

2.4.2. 1-{4-[(1,3,3-Trimethyl-1,3-dihydro-indol-2-ylidenemethyl)-azo]-phenyl}-ethanone (*4b*)

Red solid. (88%), m.p. 149.1 °C. (Found: MH^+ *m*/*z* 320.1757 $C_{20}H_{21}N_3O$ requires MH^+ *m*/*z* 320.1763; Δ = 1.9 ppm). ^1H NMR (d_6-DMSO) δ 8.02 (d, *J* 10 Hz, 2H), 7.63 (d, *J* 10 Hz, 2H), 7.51 (s, 1H), 7.46 (d, *J* 5 Hz, 1H), 7.32 (t, *J* 5 Hz, 1H), 7.18 (d, *J* 10 Hz, 1H), 7.09 (t, *J* 5 Hz, 1H), 2.58 (s, 3H), 1.53 (s, 3H), 1.71 (s, 6H). ^{13}C NMR (d_6-DMSO) δ 22.4, 26.6, 27.5, 28.6, 29.9, 34.5, 46.9, 48.0, 108.9, 120.4, 121.3, 122.0, 122.4, 126.8, 127.9, 128.1, 129.6, 134.4, 139.7, 143.8, 157.0, 168.0, 172.9, 196.8. λ_{max} (DMF) 470, $\log_{10}\varepsilon$ 4.49.

2.4.3. 6-[(1,3,3-Trimethyl-1,3-dihydro-indol-2-ylidenemethyl)-azo]-benzo[de]isoquinoline-1,3-dione (*4c*)

Green solid (72%), m.p. 235.2 °C. (Found: MH^+ *m*/*z* 397.1664 $C_{24}H_{20}N_4O_2$ requires MH^+ *m*/*z* 397.1665; Δ = 0.3 ppm). ^1H NMR (d_6-DMSO) δ 9.16 (d, *J* 5 Hz, 1H), 8.47 (t, *J* 5 Hz, 2H), 7.87 (m, 3H), 7.55 (d, *J* 10 Hz, 1H), 7.38 (m, 1H), 7.32 (d, *J* 5 Hz, 1H) 7.18 (t, *J* 5 Hz, 1H), 5.75 (s, 1H), 3.58 (s, 3H), 1.78 (s, 6H). ^{13}C NMR (d_6-DMSO) δ 28.6, 30.4, 48.7, 109.8, 110.5, 118.4, 122.2, 122.4, 123.3, 125.0, 126.1, 128.0, 128.1, 130.0, 131.1, 140.3, 143.5, 153.6, 163.9, 164.4, 170.1. λ_{max} (DMF) 545, $\log_{10}\varepsilon$ 4.60.

2.5. Preparation of compounds *4d*–*f*. General procedure for the coupling of acceptors *6d*–*f* to *4a*

Aldehyde **4a** (1 eq) and the appropriate acceptor **6d**–**f** (1.2 eq) were dissolved in methanol and a catalytic quantity of

triethylamine added. The mixture was refluxed for the period of time stated below, and resulted in a change in the colour of the solution from red to either purple or green. After cooling, the solid product was collected by filtration, washed with 3–4 times with cold methanol and dried under vacuum to give **4d**–**f** as coloured solids.

*2.5.1. 2-{4-[(1,3,3-Trimethyl-1,3-dihydro-indol-2-ylidenemethyl)-azo]-benzylidene}-malononitrile (**4d**)*

Refluxed 20 min. Violet solid (85%), m.p. 226 °C. (Found: MH^+ *m/z* 354.1722 $C_{22}H_{19}N_5$ requires MH^+ *m/z* 354.1719; Δ = 0.8 ppm). ^{1}H NMR(d_6-DMSO) δ 8.41 (s, 1H), 8.03 (d, *J* 9 Hz, 2H), 7.66 (d, *J* 9 Hz, 2H), 7.64 (s, 1H), 7.50 (d, *J* 9 Hz, 1H), 7.36 (t, *J* 6 Hz, 1H), 7.27 (d, *J* 9 Hz, 1H), 7.15 (t, *J* 6 Hz, 1H), 3.73 (s, 3H), 1.71 (s, 6H). ^{13}C (d_6-DMSO) δ 21.1, 29.0, 29.1, 30.3, 47.8, 48.6, 108.4, 109.5, 121.0, 121.2, 121.8, 122.4, 123.2, 128.4, 130.0, 131.3, 134.2, 140.2, 144.1, 158.4, 168.9. λ_{max} (DMF) 549, $\log_{10}\varepsilon$ 4.69.

*2.5.2. 3-(4-Hydroxy-phenyl)-2-thioxo-5-{4-[(1,3,3-trimethyl-1,3-dihydro-indol-2-ylidenemethyl)-azo]-benzylidene}-thiazolidin-4-one (**4e**)*

Refluxed 4 h. Green solid (75%), m.p. 220 °C. (Found: MH^+ *m/z* 513.1413 $C_{28}H_{24}N_4O_2S_2$ requires MH^+ *m/z* 513.1419; Δ = 1.2 ppm). ^{1}H NMR (d_6-DMSO) δ 9.85 (s, 1H), 7.82 (s, 1H), 7.77–7.68 (m, 4H), 7.55 (s, 1H), 7.48 (d, *J* 9 Hz, 1H), 7.33 (t, *J* 6 Hz, 1H), 7.22–7.16 (m, 3H), 7.10 (t, *J* 6 Hz, 1H), 7.68 (d, *J* 9 Hz, 2H), 3.45 (s, 3H), 1.73 (s, 3H). ^{13}C NMR (d_6-DMSO) δ 28.6, 29.9, 48.1, 109.0, 115.8, 121.4, 121.5, 122.1, 122.5, 122.8, 126.0, 128.0, 129.7, 130.9, 132.2, 132.3, 139.8, 143.8, 155.3, 158.1, 167.1, 168.0, 193.9. λ_{max} (DMF) 534, $\log_{10}\varepsilon$ 4.67.

*2.5.3. 2-[3-Cyano-5,5-dimethyl-4-(2-{4-[(1,3,3-trimethyl-1,3-dihydro-indol-2-ylidenemethyl)-azo]-phenyl}-vinyl)-5H-furan-2-ylidene]-malononitrile (**4f**)*

Refluxed 2 h. Green solid (80%), m.p. 275 °C. (Found: MH^+ *m/z* 487.2247 $C_{30}H_{26}N_6O$ requires MH^+ *m/z* 487.2246; Δ = 0.2 ppm). ^{1}H NMR (d_6-DMSO) δ 7.98 (d, *J* 9 Hz, 2H), 7.94 (s, 1H), 7.65 (d, *J* 9 Hz, 2H), 7.62 (d, *J* 15 Hz, 1H), 7.48 (d, *J* 6 Hz, 1H), 7.34 (t, *J* 5 Hz, 1H), 7.22 (d, *J* 6 Hz, 1H), 7.17 (d, *J* 15 Hz, 1H), 7.12 (t, *J* 5.5 Hz, 1H), 3.47 (s, 3H), 1.81 (s, 6H), 1.72 (s, 6H). ^{13}C NMR (d_6-DMSO) δ 25.2, 28.4, 30.0, 48.2, 99.1, 109.1, 112.8, 113.9, 121.2, 122.0, 122.6, 123.1, 127.9, 131.0, 147.1, 175.0. λ_{max} (DMF) 601, $\log_{10}\varepsilon$ 5.04.

*2.6. Preparation of compounds **4g**,**h**. General procedure for the coupling of acceptors **6g**,**h** to **4a***

Aldehyde **4a** (1 eq) and the appropriate salt (1.1 eq) were dissolved in methanol and a catalytic quantity of triethylamine was added. The reaction mixture was refluxed for 18 h and this resulted in a change in the colour of the mixture from red to brown. After the reaction was completed 75% of the solvent was removed at reduced pressure and ether added until a solid appeared. This was collected by filtration, washed with 3–4 times with cold ethanol and dried under vacuum to give **4g**,**h** as coloured solids.

*2.6.1. 2-[2-(2-{4-[(1,3,3-Trimethyl-1,3-dihydro-indol-2-ylidenemethyl)-azo]-phenyl}-vinyl)-benzothiazol-3-yl]-ethanol iodide (**4g**)*

Greenish-red solid (72%), m.p. 259–63 °C (dec.). (Found: M^+ *m/z* 481.2116 $C_{29}H_{29}N_4OS$ requires M^+ *m/z* 481.2113; Δ = 0.6 ppm). ^{1}H NMR (d_6-DMSO) δ 8.25 (d, *J* 15 Hz, 1H), 7.98 (d, *J* 9 Hz, 2H), 7.82 (s, 1H), 7.62 (d, *J* 9 Hz, 2H), 7.51 (d, *J* 9 Hz, 1H), 7.38 (t, *J* 6 Hz, 1H), 7.26–7.22 (m, 3H), 7.15 (t, *J* 6 Hz, 1H), 6.98 (d, *J* 15 Hz, 1H), 6.82–6.78 (m, 2H), 5.07 (t, *J* 6 Hz, 2H), 4.50 (t, *J* 6 Hz, 2H), 3.45 (s, 3H), 1.73 (s, 6H). ^{13}C NMR (d_6-DMSO) δ 12.8, 14.2, 27.3, 32.1, 44.5, 45.8, 50.0, 54.9, 112.0, 113.8, 116.6, 118.4, 122.5, 124.2, 125.7, 128.2, 128.3, 128.5, 128.9, 129.5, 131.3, 131.9, 140.9, 141.2, 143.0, 148.5, 171.2. λ_{max} (DMF) 567, $\log_{10}\varepsilon$ 4.48.

*2.6.2. 2-[4-(2-{4-[(1,3,3-Trimethyl-1,3-dihydro-indol-2-ylidenemethyl)-azo]-phenyl}-vinyl)-quinolin-1-yl]-ethanol iodide (**4h**)*

Dark brown solid (70%), m.p. 249–252 °C (dec.). (Found: M^+ *m/z* 475.2504 $C_{31}H_{31}N_4O$ requires M^+ *m/z* 475.2498; Δ = 1.3 ppm). ^{1}H NMR (d_6-DMSO) δ 9.10 (d, *J* 9 Hz, 1H), 9.08 (d, *J* 9 Hz, 1H), 8.25 (d, *J* 15 Hz, 1H), 8.20 (m, 2H), 7.94 (d, *J* 9 Hz, 2H), 7.60 (d, *J* 9 Hz, 2H), 7.86 (m, 2H), 7.80 (s, 1H), 7.48 (d, *J* 6 Hz, 1H), 7.34 (t, *J* 5 Hz, 1H), 7.22 (d, *J* 6 Hz, 1H), 7.12 (t, *J* 6 Hz, 1H), 6.98 (d, *J* 15 Hz, 1H), 5.07 (t, *J* 5 Hz, 2H), 4.50 (t, *J* 5 Hz, 2H), 3.45 (s, 3H), 1.73 (s, 6H). ^{13}C NMR (d_6-DMSO) δ 28.6, 29.9, 48.1, 109.0, 115.8, 121.4, 121.5, 122.1, 122.5, 122.8, 126.0, 128.0, 129.7, 130.9, 132.2, 132.3, 139.8, 143.8, 155.3, 158.1, 167.1, 168.0, 193.9. λ_{max} (DMF) 555, $\log_{10}\varepsilon$ 4.03.

*2.7. Synthesis of 2-(3-dicyanomethylene-5,5-dimethyl-2-{4-[(1,3,3-trimethyl-1,3-dihydro-indol-2-ylidenemethyl)-azo]-benzylidene}-cyclohexylidene)-malononitrile (**4i**)*

To a mixture of aldehyde **4a** (10 mmol, 3.05 g) and dimedone (10 mmol, 1.40 g) in toluene was added triethylamine (10 mmol, 1.0 mL). The reaction mixture was refluxed for 10 h and the water generated removed using a Dean–Stark trap. After all the starting materials had been consumed (via TLC) malononitrile (20 mmol, 1.32 g) was added and the reaction mixture refluxed for a further 4 h resulted. This resulted in a colour change from red to brownish red. The solvent was removed under reduced pressure, extracted into dichloromethane, and washed with water. The organic phase was then dried ($MgSO_4$) and concentrated. The resultant solid was purified by column chromatography (using dichloromethane as eluent) to give a dark brownish-red solid. (45%), m.p. 136.2 °C. (Found: MH^+ *m/z* 523.2533 $C_{33}H_{29}N_7$ requires MH^+ *m/z* 523.2538; Δ = 1.2 ppm). ^{1}H NMR (d_6-DMSO) δ 8.47 (s, 1H), 8.09 (d, *J* 9 Hz, 2H), 7.70 (d, *J* 9 Hz, 2H), 7.64 (s, 1H), 7.50 (d, *J* 9 Hz, 1H), 7.36 (t, *J* 5 Hz, 1H), 7.27(d, *J* 9 Hz, 1H), 7.15 (t, *J* 5 Hz, 1H), 3.73 (s, 3H), 1.90 (s, 4H), 1.71 (s, 6H), 1.50 (s, 6H). ^{13}C (d_6-DMSO) δ 21.1, 24.8, 27.7, 29.0, 29.1, 30.2, 48.5, 77.4, 109.5, 114.9, 121.1, 121.5, 122.1, 123.1, 123.7, 128.0, 125.7, 132.5, 140.6, 158.2, 159.9, 168.9, 169.4. λ_{max} (DMF) 441, $\log_{10}\varepsilon$ 4.33.

3. Results and discussion

3.1. Synthesis

The structures of the molecules prepared for this study are shown in Fig. 1. The chromophores can be classified as one of two types depending on the synthetic methodology used to prepare them. The first type are chromophores **4a**–**c**, and which were obtained in one step by simply coupling the corresponding diazonium salt, **6a**–**c**, to Fischer's base **5** (Scheme 1). The reactions employed standard conditions for the diazotization of the appropriate aryl amine in glacial acetic acid. These diazonium couplings proceeded in high yield (72–88%) and this reinforces the strong electron donating ability of the indoline ring system. Compound **4a** is the key synthon for the preparation of chromophores **4d**–**i**, and so was synthesised in multi-gram quantities. Compounds **4d**–**h** could then be obtained by refluxing **4a** and the appropriate acceptor **6d**–**h** for between 20 min and 24 h in methanol containing a catalytic amount of triethylamine (Scheme 2). A key advantage of the methodologies used to prepare **4a**–**h** is that it was not necessary to perform chromatography in order to obtain the final products pure. Compound **4i** was obtained by first condensing **4a** with dimedone in refluxing toluene and then adding malononitrile to the reaction mixture and heating for an additional 5 h. The structures of all the

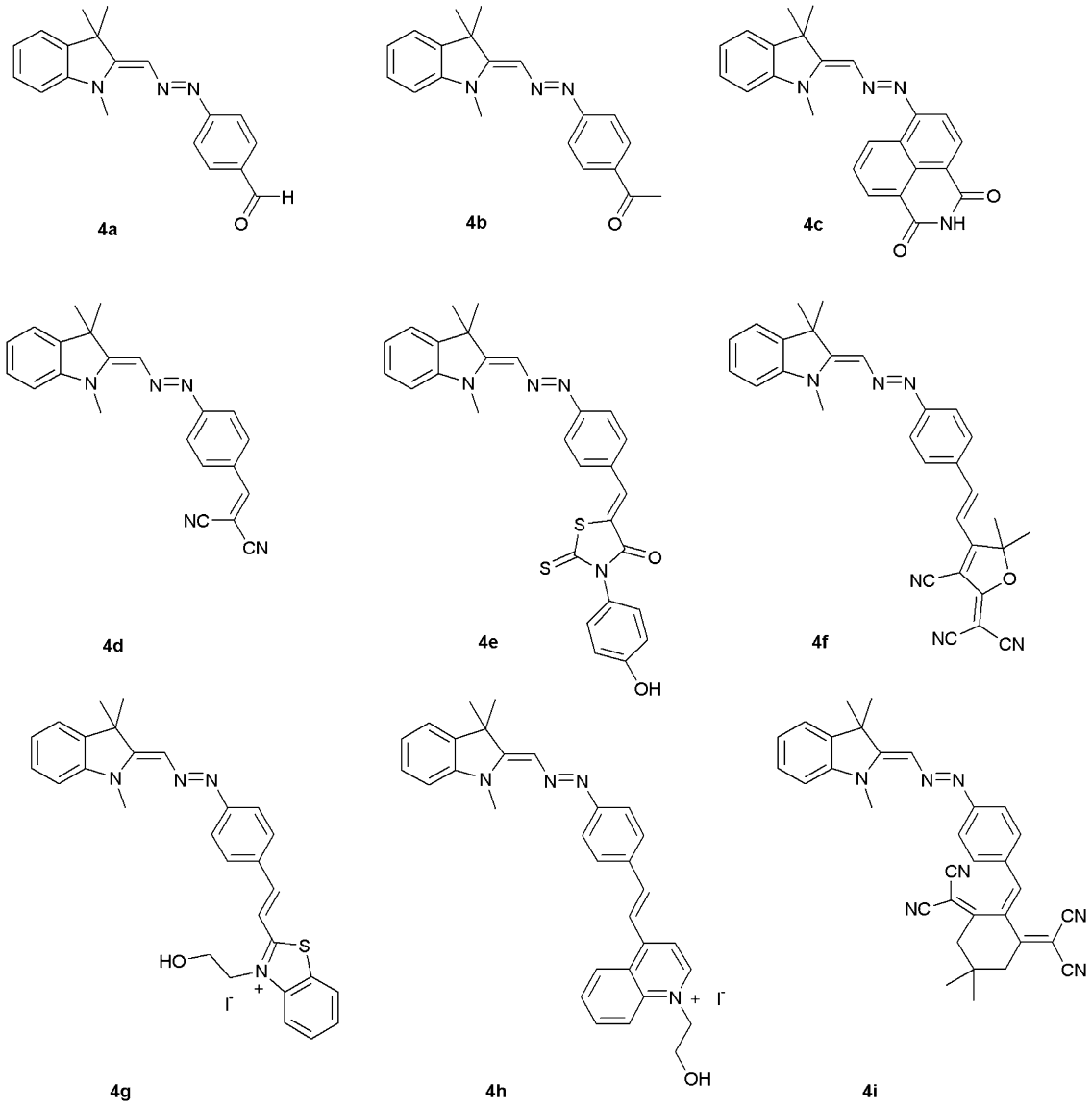

Fig. 1. Structures of the compounds prepared in this study.

chromophores were confirmed by ^{1}H and ^{13}C NMR, UV–vis spectroscopy and high resolution mass spectrometry. The azo linkers are all assumed to be in the *trans*-configuration, and for compounds **4f**–**h** the double bonds adjacent to acceptor rings are also expected to be in a *trans*-configuration and evidenced by the large coupling constants of 15 Hz observed in the NMR spectra. The thermal decomposition temperatures (T_d) of all chromophores were measured by differential scanning calorimetry and the results are presented in Table 2. Importantly, all the chromophores, with the

Table 1
UV–Visible spectroscopic data for the compounds prepared in this study.

Compound	λ_{max}, THF (nm)	$Log_{10}\varepsilon$, (THF)	λ_{max}, DMF (nm)	$Log_{10}\varepsilon$, (DMF)	λ_{max}, PYR (nm)	$\Delta\lambda_{max}$, DMF-PYR (nm)
4b	461	4.49	470	4.49	471	−1
4c	531	4.66	545	4.60	544	1
4d	540	4.95	549	4.69	460	91
4e	525	4.79	534	4.67	540	−6
4f	590	4.75	601	5.04	440	161
4g	574	3.95	567	4.48	445	122
4h	551	3.75	555	4.03	435	120
4i	429	4.53	441	4.33	436	5

Table 2
Dynamic first hyperpolarizability β_{zzz} values determined at a fundamental wavelength of 800 nm; static hyperpolarizability $\beta_{zzz,0}$ values derived with the two level model and decomposition temperatures of the compounds prepared in this study.

Compound	Solvent	β_{zzz} ($*10^{-30}$ esu)	Average β_{zzz} ($*10^{-30}$ esu)	$\beta_{zzz,0}$ ($*10^{-30}$ esu)	Average $\beta_{zzz,0}$ ($*10^{-30}$ esu)	T_d (°C)
4b	THF	325 ± 30	270 ± 20	70 ± 6	60 ± 5	254
	DMF	210 ± 10		50 ± 3		
4c	THF	470 ± 15	425 ± 20	200 ± 5	185 ± 10	220
	DMF	375 ± 20		170 ± 10		
4d	THF	710 ± 20	630 ± 25	320 ± 10	290 ± 10	230
	DMF	550 ± 25		260 ± 10		
4e	THF	695 ± 25	675 ± 25	290 ± 10	285 ± 10	245
	DMF	650 ± 25		280 ± 10		
4f	THF	1060 ± 55	1350 ± 105	570 ± 30	735 ± 60	270
	DMF	1640 ± 155		900 ± 85		
4g	THF	640 ± 35	630 ± 40	330 ± 20	320 ± 20	234
	DMF	620 ± 45		310 ± 20		
4h	THF	350 ± 30	350 ± 25	165 ± 15	165 ± 15	230
	DMF	345 ± 20		165 ± 10		
4i	THF	430 ± 20	390 ± 20	46 ± 2	50 ± 3	171
	DMF	350 ± 20		55 ± 3		

exception of **4i**, have decomposition temperatures above 230 °C, which suggests they will be amenable to poling at high temperatures. The best performing chromophore, **4f**, has a T_d value of 270 °C which is close to that of the well-known NLO material, 4-dimethylamino-4′-nitrostilbene (DANS) (T_d, 290 °C) [22].

3.2. Linear optical properties

The absorption maxima and molar extinction coefficients for chromophores **4b**–**i** are given in Table 1, and cover a range of solvents with varying dielectric constants, i.e. tetrahydrofuran (THF, $\varepsilon = 7.5$), pyridine (PYR, $\varepsilon = 12.4$) and *N*,*N*-dimethylformamide (DMF, $\varepsilon = 38$). The main absorption bands are located in the ranges of 429–590 nm (THF), 435–544 nm (PYR) and 441–601 nm (DMF). These bands are attributable to intramolecular charge-transfer (ICT) transitions, and it is seen that with THF and DMF as solvent that compound **4i** has the highest energy absorption while for the same solvents compound **4f** has the lowest energy absorption maxima. Based on previous observations that compounds with the lowest energy absorption maxima typically have the highest NLO response [1], it would be expected that compound **4f** will have the highest first hyperpolarizability, β, of the series. Furthermore, with the exception of **4g**, upon changing the solvent from the less polar THF to DMF there is an approximate 10 nm bathochromic shift in the absorption maxima. This positive solvatochromic shift implies that the excited states of the compounds are more polar than the ground states and is consistent with what would be expected for chromophores containing a indoline – and indeed a *N*,*N*-disubstituted aniline-donor unit. The anomalous behaviour seen for **4g** is probably due to the benzothiazolium "acceptor" nucleus also being able to act as a donor and this presumably results in a reversal of the ground state polarity. With pyridine as solvent there is no clear trend as some compounds show a hypsochromic or bathochromic shift in their absorption maximum with respect to the value found in DMF. This reflects the somewhat complex nature of solvent–solute interactions plus the fact that solvatochromism can be influenced by a number of factors such as solvent polarity and a solvent's H-bond donor/acceptor ability – these in turn can affect the solvation energy of a given compound and lead to significant variations in the absorption maximum [23]. Nonetheless from the data presented in Table 1 it is very clear that for some compounds, *viz.* **4d**, **4f**–**4h**, the most significant hypsochromic shifts occur when comparing the absorption maxima obtained in DMF with those obtained in pyridine, with the largest change being 161 nm for compound **4f**. As a general rule of thumb, compounds that exhibit high degrees of solvatochromism (i.e. $\Delta\lambda > 100$ nm) also have a large second-order NLO responses. Consequently, based purely on UV–Vis data, **4f**, with the well-studied TCF acceptor, is predicted to have a large first hyperpolarizability.

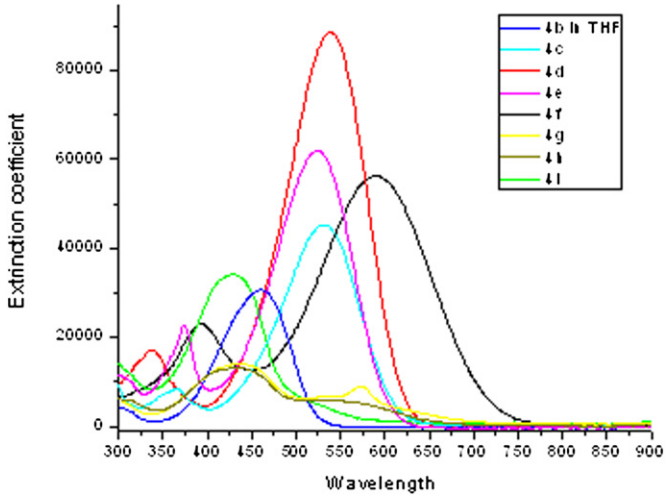

Fig. 2. UV–Vis spectra of compounds **4b**–**i** in THF.

It is also worth noting that when the UV–vis spectra are obtained in the solvent with the lowest polarity, THF, there is no evidence for either H- or J-aggregation (Fig. 2). The former is identifiable through the appearance of a high energy shoulder on the main absorption band, while the latter is characterised though the presence of a low energy shoulder. This therefore suggests that there is only a very small degree of charge separation in the ground state of the molecules, as a moderate degree of zwitterionic character would almost certainly manifest itself via the appearance of high or low energy shoulders [24]. The absence of any evidence for aggregation is encouraging as, in order to be usefully deployed, these chromophores need to be both non-centrosymmetrically aligned in a polymer matrix (via electric field poling) and this alignment maintained indefinitely. As the dielectric constant of THF is within the range found for most polymers, i.e. 1–7 [25] this suggests that these compounds will respond well to the poling process and that the temporal stability post-poling will be less affected.

3.3. Quadratic nonlinear optical properties

The quadratic optical nonlinearities of compounds **4b**–**i** were determined using the Hyper-Rayleigh scattering (HRS) technique at 800 nm employing femtosecond (fs) pulses. The second-order NLO polarizability (or first hyperpolarizability β_{zzz}) and the static first hyperpolarizability $\beta_{zzz,0}$ of all the compounds under investigation are listed in Table 2. It should be noted that there is no fluorescence contribution from any of the compounds. The differences in second-order NLO response between the various compounds can be explained using the two level model developed by the Oudar and Chemla, equation (1) [19a]. According to this model, β is directly proportional to the difference in the dipole moment between the highest occupied (HOMO) and the lowest unoccupied (LUMO) molecular orbitals ($\Delta\mu_{eg}$) and the transition dipole moment (oscillator strength) (μ_{ge}). The model also states that β is inversely proportional to the energy difference between ground state (HOMO) and charge transferred excited state (LUMO) E_{ge}. Thus, any phenomenon that decreases this energy gap and increases the dipole moment difference between the ground and the excited states will enhance β.

$$\beta_{zzz}\alpha\frac{\Delta\mu_{eg}(\mu_{ge})^2}{E_{ge}^2} \quad (1)$$

From the results presented in both Tables 1 and 2 the magnitude of the β_{zzz} and $\beta_{zzz,0}$ responses are in general agreement with the values expected from the linear optical properties. Thus, those compounds with the lowest energy absorption maxima exhibit the highest nonlinear optical responses. The highest dynamic response (1640×10^{-30} esu) was found for compound **4f** in DMF (λ_{max} 601 nm) while the lowest value (210×10^{-30} esu) was recorded for **4b**, also in DMF (λ_{max} 470 nm). As has been well documented in the past, while the NLO response will depend on a variety of structural/electronic factors including donor/acceptor strength and the extent of conjugation, differences in solvent polarity as well as the fundamental wavelength used to make the measurements can also have a significant impact. We have previously described how changes in solvent polarity can impact on the observed response

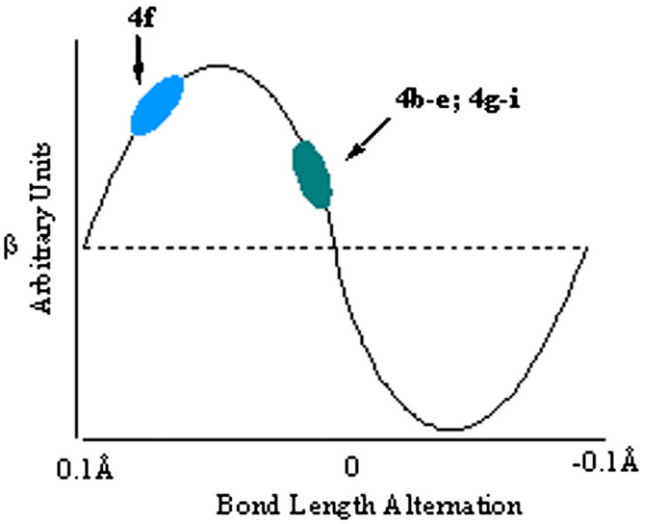

Fig. 3. Relationship between hyperpolarizability and bond length alternation for NLO chromophores. The ellipsoids represent where, approximately, hyperpolarizability data suggests the various compounds used in this study sit on the curve.

for a series of chromophores containing donors based on 1,4-dihydropyridine and 1,4-dihydroquinoline [26]. Such changes are due to the relationship between bond length alternation (BLA) in the chromophore and the inherent hyperpolarizability [8]. Furthermore, depending on where a given molecule sits on the theoretical BLA vs β sinusoidal curve can result in either an increase or decrease in the observed hyperpolarizability (Fig. 3). Given that the current molecules have only a very small degree of zwitterionic character they can be defined as "left hand side molecules" and this means that any increase in the polarity of the solvent leads to an increase in charge separation and a shift in BLA towards zero. In the present case, all of the compounds with the exception of the best performing compound **4f**, have a superior dynamic NLO response in the less polar solvent THF ($\varepsilon = 7.5$). Consequently this would suggest that, as depicted in Fig. 3, only **4f** sits to the left of the theoretical β vs BLA maximum. Furthermore, the result implies that deployment of **4f** in the low polarity environments often found in polymers will result in a reduction in the macroscopic NLO response. Nonetheless, as the magnitudes of both the static and dynamic hyperpolarizabilities of **4f** in THF are still significantly higher than any of the other compounds in the same solvent it is clearly the superior molecule.

Table 4
Selected bond distances (Å) in **4e**.

Bond	A	B (primed)
N_2–N_3	1.325 (11)	1.311 (11)
C_{12}–N_2	1.382 (11)	1.395 (12)
N_3–C_{13}	1.417 (12)	1.406 (12)
C_{19}–C_{20}	1.409 (13)	1.409 (14)
S_1–C_{20}	1.707 (11)	1.730 (12)
S_1–C_{22}	1.766 (11)	1.759 (11)
C_{22}–S_2	1.604 (11)	1.591 (12)
C_{26}–O_2	1.435 (12)	1.410 (14)

It is also worth making a comparison of the relative merits of using an indoline versus a more conventional aniline based donor. As mentioned earlier the β and β_0 values reported for the known *N*,*N*-dimethylaminophenyl analogue of **4f** (Fig. 1) in DMSO ($e = 46.7$) are 682 and 343 $\times$ 10^{-30} esu respectively; these measurements were also performed using a laser with fundamental wavelength of 800 nm [16]. These values are considerably lower than those of the indoline derivative **4f** (1640 and 900 $\times$ 10^{-30} esu in DMF; $\varepsilon = 38$) even taking into account the modest differences in solvent polarity. Therefore, this indicates that NLO chromophores based on indoline donors could be capable of a similar, if not better, performance than those that employ an aniline based donor. However, as the current results are based on a single comparison more detailed studies are clearly required to confirm this conclusion.

3.4. X-ray crystallography

We have managed to obtain adequate X-ray crystallographic data for compound **4e** and a selection of results are presented in Tables 3 and 4. While crystallographic data for the more effective compound, **4f**, would have been preferred, we were unable to grow suitable crystals due to twinning. Nonetheless, the X-ray data obtained for **4e** provides valuable insight into molecular interactions, and these in turn relate to the ease by which a non-centrosymmetric alignment can be obtained by poling. Table 3 contains the refinement data whereas Table 4 contains a summary of key bond lengths. The crystals are packed in a centrosymmetric fashion and contain solvents of crystallization (Table 3).

Table 3
Crystallographic and structure refinement data for **4e**.

Asymmetric unit	C_{62} H_{66} N_4 O_7 S_4	μ, mm^{-1}	1.96
Moiety formula	$2(C_{28}$ H_{24} N_2 O_2 $S_2)0.2(C_3H_8O)\cdot H_2O$	Limiting indices	$-11 \le h \le 10$, $0 \le k \le 31$, $0 \le l \le 17$
MW	1163.47	Crystal size (mm)	0.63 $\times$ 0.20 $\times$ 0.08
Temperature (K)	153 (2)	Theta range °	6.5–50.4
Wavelength (Å)	1.54178	Reflections collected	10352
Crystal system,	Monoclinic	No of unique data	5232
Space group	$P2_1/n$	R_{int}	0.087
Refinement method	Full matrix least-squares on F^2	*P*1,*P*2 coefficients of weighting scheme[a]	0.1898,
a, Å	11.2224 (19)	Absorp. Coeff. range	0.507, 1.0
b, Å	31.855 (3)	Restraints	3
c, Å	17.0522 (6)	No. of parameters	393
β, °	103.926 (8)	Goodness-of-fit on F^2	0.90
Volume, $Å^3$	5916.8 (13)	R_1[b,c], /data number	0.110, 1743
Z	4	wR_2[c] i (all data)	0.339
P, Mg m^{-3}	1.306	Largest diff. peak and hole (e A^{-3})	0.33 and−0.37

[a] Weight, $w = 1/[\sigma^2(F_o^2) + (P1^*P)^2]$ where $P = (\text{Max}\ (F_o^2, 0) + 2^*F_c^2)/3$.
[b] Intensities 2.0 times their standard deviations (from counting statistics).
[c] $R_1 = \Sigma||F_o|-|F_c||/\Sigma|F_o|$; $wR_2 = \Sigma[w\ (F_o^2-F_c^2)^2]/\Sigma[(wF_o^2)^2]^{1/2}$.

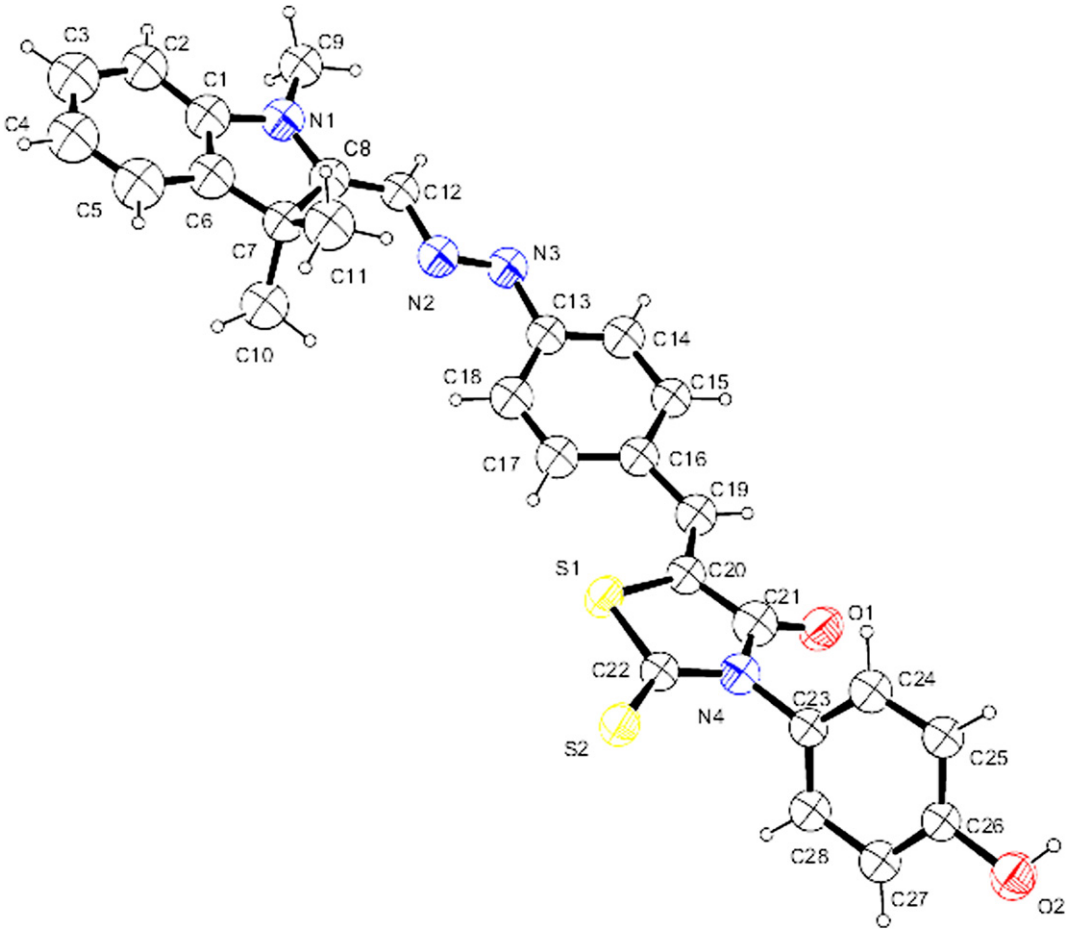

Fig. 4. Structure of molecule A in **4e** (with 20% probability ellipsoids) [29].

*3.4.1. Crystallographic features of compound **4e***

The asymmetric unit of **4e** contains two independent copies of the compound (Fig. 4 shows one of them, A; molecule B has identical primed labels) and three solvate molecules: one water and two 2-propanol molecules. Excluding the terminal 4-hydroxy-phenyl ring, the molecules are approximately planar lying parallel to the (1, 0, 1) plane. The terminal 4-hydroxy-phenyl rings make angles of 76.3 (6)° (in A, shown in Fig. 4) and 85.9 (6)° (B) to the 5-membered thioxo rings (S1, C20–C22, N4). The root mean square bond and angle fits between the two molecules are 0.031 Å and 2.20° [27]. The molecules are not exactly superimposable with molecule A twisting further from planarity around the central C13–C18 ring: the interplanar angles with the 5-membered thiooxo rings are 20.5 (6)° and 6.5 (6)° respectively (molecules A & B). The molecular contents are bound together via O–H···O, O–H.···N(azo) and C–H···O interactions (Table 5, Fig. 5 shows some of these interactions). The water (O7) hydrogens were refined from calculated positions but other alternative positions are possible; data resolution is insufficient to be definitive. It seems most likely that two independent adjacent parallel molecules are bound in a bifurcated manner to the water O7 via O7–H···N3(azo) interactions, with the water oxygen also acting as acceptor from the 2-propanol hydroxyl protons. Molecules lying "side by side" are linked by weaker C–H···O(=C) interactions completing $R_2^2(10)$ and $R_2^2(12)$ motifs [28]. The overall packing is thus based on a full 3-dimensional interaction set through the solvate molecule interactions, and suggests that dipole alignment via poling will require reasonably high voltages.

Table 5
Hydrogen bond geometry (Å, °) for **4e**.

D–H···A	D–H	H···A	D···A	D–H···A	Symmetry[a]
O2′–H2O···O6	0.85 (13)	1.87 (15)	2.577 (15)	140 (10)	$1-x, -y, 1-z$
O2–H2O···O5	0.84	1.78	2.611 (12)	168	$1+x, 1+y, z$
O5–H5O···O7	0.84	1.96	2.699 (14)	146	$x-0.5, 0.5-y, 0.5+z$
O7–H1O7···O6	0.84 (7)	2.19 (14)	2.696 (13)	119 (13)	x, y, z
O7–H2O7···N3	0.85 (11)	2.54 (14)	2.806 (13)	100 (8)	$1-x, 1-y, 1-z$
C5–H5···O2′	0.95	2.57	3.491 (19)	164	$0.5x, 0.5-y, z-0.5$
C5′–H5′···O2	0.95	2.55	3.495 (14)	171	$x-0.5, 1.5-y, 0.5z$
C19–H19···O1′	0.95	2.41	3.345(14)	166	$x, 1y, z$
C19′–H19′···O1	0.95	2.32	3.172(14)	149	$x, y-1, z$

[a] Symmetry to bring the A atom into contact.

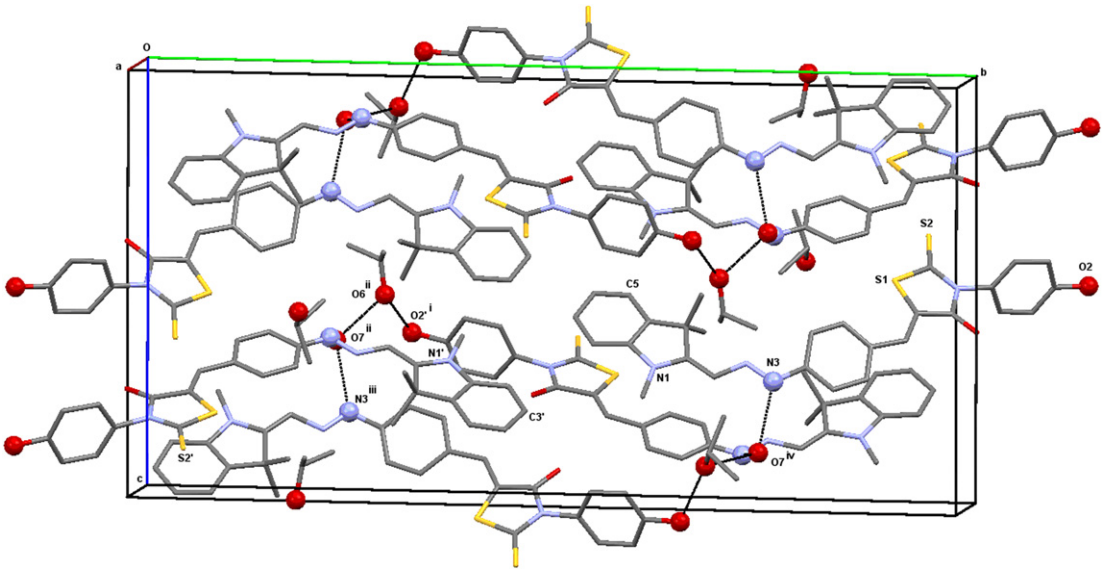

Fig. 5. Crystal packing of **4e** [30]; some of the main attractive contacts are shown as dotted lines (see Table 5). Symmetry (i): $1.5 - x, 0.5 + y, 1.5 - z$ (ii) $0.5 + x, 0.5 - y, 0.5 + z$ (iii) $1.5 - x, y - 0.5, 1.5 - z$ (iv) $1 - x, 1 - y, 1 - z$.

4. Summary and conclusions

A series of push–pull azo-based chromophores, derived from an indoline donor have been synthesized using a straightforward synthetic protocol. UV–Vis spectra of the compounds show no evidence of aggregation in solution and in some cases the chromophores exhibit high degrees of solvatochromism ($\Delta\lambda > 100$ nm). An X-ray crystallographic study of one chromophore, **4e**, has been undertaken in order to provide structural details for one compound. The static and dynamic first hyperpolarizabilities at 800 nm were obtained, and chromophore **4f** – which contains the well-studied TCF acceptor – was found to have the highest response in both polar and nonpolar media. Furthermore a comparison of the values obtained for **4f** with its equivalent aniline-based derivative suggests indoline donors are capable of yielding compounds with very high NLO responses. Consequently further studies are underway to investigate the properties of other chromophores containing an indoline donor with a view to making meaningful comparisons with their aniline-based analogues.

Acknowledgements

This work has been supported by the New Zealand Ministry for Science and Innovation (Contract C08X0704) and by grants from the University of Leuven (GOA/2006/03).

References

[1] Kay A, Woolhouse A, Zhao Y, Clays K. Synthesis and linear/nonlinear optical properties of a new class of 'RHS' NLO chromophore. Journal of Materials Chemistry 2004;14:1321–30.
[2] Bass M, Enoch JM, Stryland EWV, Wolfe WL, editors. Handbook of optics IV, fibre optics and nonlinear optics. New York: Academic Press; 2001.
[3] Prasad PN, Ulrich DR, editors. Nonlinear optical and electroactive polymers. New York: Plenum; 1988.
[4] Burland DM, Miller RD, Walsh CA. Second-order nonlinearity in poled-polymer systems. Chemical Reviews 1994;94:31–75.
[5] Dalton LR, Sullivan PA, Bale D, Olbricht B, Davies J, Benight S, et al. Organic electro-optic materials. In: Organic thin films for photonic applications. Washington DC: American Chemical Society; 2010.
[6] Liu S, Haller MA, Ma H, Dalton LR, Jang SH, Jen AKY. Focused microwave-assisted synthesis of 2,5-dihydrofuran derivatives as electron acceptors for highly efficient nonlinear optical chromophores. Advanced Materials 2003;15:603–7.
[7] (a) Dalton LR, Benight SJ, Johnson LE, Knorr DB, Kosilkin I, Eichinger BE, et al. Systematic nanoengineering of soft matter organic electro-optic materials. Chemistry of Materials 2011;23:430–45;
(b) Cho MJ, Choi DH, Sullivan PA, Akelaitis AJP, Dalton LR. Recent progress in second-order nonlinear optical polymers and dendrimers. Progress in Polymer Science 2008;33:1013–58.
[8] Marder SR, Cheng LT, Tiemann BG, Friedli AC, Blanchard-desce M, Perry JW, et al. Large first hyperpolarizabilities in push–pull polyenes by tuning of the bond length alternation and aromaticity. Science 1994;263:511–4.
[9] (a) . In: Chemla DS, Zyss J, editors. Nonlinear optical properties of organic molecules and crystals, vols. 1 and 2. New York: Academic Press; 1987;
(b) Williams DJ. Organic polymeric and non-polymeric materials with large optical nonlinearities. Angewandte Chemie International Edition in English 1984;23:690–703.
[10] Cheng L-T, Tam W, Feiring AE, Rikken GL. Nonlinear optical properties of organic nonlinear materials. SPIE Proceedings 1990:1337.
[11] Kuzyk MG, Dirk CW, editors. Characterization techniques and tabulation for organic nonlinear optical materials. New York: Academic Press; 1998.
[12] (a) Moylan CR, Swanson SA, Walsh CA, Thakara JI, Twieg RJ, Miller RD, et al. From electric field-induced second harmonic generation (EFISH) to electro-optic measurements of nonlinear chromophores. SPIE Proceedings 1993:2025;
(b) Cui Y, Qian G, Chen L, Wang Z, Wang M. Synthesis and nonlinear optical properties of a series of azo chromophore functionalized alkoxysilanes. Dyes and Pigments 2008;77:217–22;
(c) Li Z, Yu G, Liu Y, Ye C, Qin J, Li Z. Dendronized polyfluorenes with high azo-chromophore loading density: convenient synthesis and enhanced second-order nonlinear optical effects. Macromolecules 2009;42:6463–72.
[13] Parsanasab GM, Sharbati MT, Karimi-Alavijeh HR, Soltani S, Gharavi A. Integrated polymeric all-optical switch. Journal of Lightwave Technology 2010;29(18):2801–4.
[14] Ono H, Takahashi F, Emoto A, Kawatsuki N. Polarization holograms in azo dye-doped polymer dissolved liquid crystal composites. Journal of Applied Physics 2005;97(5). p. 053508-1–053508-8.
[15] Gallego-Gómez F, del Monte F, Meerholz K. Optical gain by a simple photo-isomerization process. Nature Materials 2008;7:490–7.
[16] Qiu L, Shen Y, Hao J, Zhai J, Zu F, Zhang T, et al. Study on novel second-order NLO azo-based chromophores containing strong electron-withdrawing groups and different conjugated bridges. Journal of Materials Science 2004;39:2335–40.
[17] Bhuiyan MDH, Ashraf M, Teshome A, Gainsford GJ, Kay AJ, Asselberghs I, et al. Synthesis, linear & nonlinear optical (NLO) properties of some indoline based chromophores. Dyes and Pigments 2011;89:177–87;
(b) Bhuiyan MDH, Teshome A, Gainsford GJ, Ashraf M, Clays K, Asselberghs I, et al. Synthesis, characterization, linear and nonlinear optical (NLO) properties of some Schiff's bases. Optical Materials 2010;32:669–72.
[18] (a) Perez-Moreno J, Zhao Y, Clays K, Kuzyk MG. Modulated conjugation as a means for attaining a record high intrinsic hyperpolarizability. Optics Letters 2007;32:59–61;
(b) Perez-Moreno J, Zhao Y, Clays K, Shen Y, Qiu L, Hao J, et al. Modulated

conjugation as a means for improving the intrinsic hyperpolarizability. Journal of the American Chemical Society 2009;131:5084–93.
[19] (a) Oudar JL, Chemla DS. Hyperpolarizabilities of the nitroanilines and their relationship to the excited state dipole moment. Journal of Chemical Physics 1977;66:2664–8;
(b) Zyss J, Oudar JL. Structural dependence of nonlinear-optical properties of methyl-(2,4-dinitrophenyl)-aminopropanoate crystals. Physical Review A 1982;26:2016–27.
[20] (a) Olbrechts G, Munters T, Clays K, Persoons A, Kim O-K, Choi L-S. High-frequency demodulation of multi-photon fluorescence in hyper-Rayleigh scattering. Optical Materials 1999;12:221–4;
(b) Olbrechts G, Strobbe R, Clays K, Persoons A. High-frequency demodulation of multi-photon fluorescence in hyper-Rayleigh scattering. Review of Scientific Instruments 1998;69:2233–41.
[21] (a) Gopalan P, Katz HE, McGee DJ, Erben C, Zielinski T, Bousquet D, et al. Star-shaped azo-based dipolar chromophores: design, synthesis, matrix compatibility, and electro-optic activity. Journal of the American Chemical Society 2004;126:1741–7;
(b) Kay AJ, Woolhouse AD, Gainsford GJ, Haskell TG, Wyss CP, Giffin SM, et al. Simple zwitterionic merocyanines as potential NLO chromophores. Journal of Materials Chemistry 2001;11:2271–81;
(c) Kay AJ, Woolhouse AD, Gainsford GJ, Haskell TG, Barnes TH, McKinnie IT, et al. A simple, novel method for the preparation of polymer-tetherable, zwitterionic merocyanine NLO-chromophores. Journal of Materials Chemistry 2001;11:996–1002;
(d) Melikian G, Rouessac F, Alexandre C. Synthesis of substituted dicyanomethylendihydrofurans. Synthetic Communications 1995;25:3045–51.
[22] Christopher RM, Robert JT, Victor YL, Sally AS, Kathleen MB, Robert DM. Nonlinear optical chromophores with large hyperpolarizabilities and enhanced thermal stabilities. Journal of the American Chemical Society 1993; 115:12599–600.
[23] Gorman AA, Hutchings MG, Wood PD. Solvatochromism of an amino-benzodifuranone: an unprecedented positive wavelength shift. Journal of the American Chemical Society 1996;118:8497–8.
[24] Teshome A, Kay AJ, Woolhouse AD, Clays K, Asselberghs I, Smith GJ. Strategies for optimising the second-order nonlinear optical response in zwitterionic merocyanine dyes. Optical Materials 2009;31:575–82.
[25] Abbotto A, Beverina L, Bradamante S, Facchetti A, Klein C, Pgani GA, et al. A distinctive example of the cooperative interplay of structure and environment in tuning of intramolecular charge transfer in second-order nonlinear optical chromophores. Chemistry – A European Journal 2003;9:1991–2007.
[26] Smith GJ, Middleton AP, Clarke DJ, Teshome A, Kay AJ, Bhuiyan MDH, et al. The effect of solvent on the excited states and first hyperpolarizability of "push–pull" merocyanines. Optical Materials 2010;32:1237–43.
[27] Spek AL. Single-crystal structure validation with the program PLATON. Journal of Applied Crystallography 2003;36:7–13.
[28] Bernstein J, Davis RE, Shimoni L, Chang N-L. Patterns in hydrogen bonding: functionality and graph set analysis in crystals. Angewandte Chemie International Edition in English 1995;34:1555–73.
[29] Farrugia LJ. *ORTEP*-3 for windows – a version of *ORTEP*-III with a graphical user interface (GUI). Journal of Applied Crystallography 1997;30:565.
[30] Macrae CF, Bruno IJ, Chisholm JA, Edgington PR, McCabe P, Pidcock E, et al. Mercury CSD 2.0-new features for the visualization and investigation of crystal structures. Journal of Applied Crystallography 2008;41:466–70.